# Impact of Phase Displacement among Coupled Inverters on Harmonic Distortion in MicroGrids

Rasul Hemmati, Reza Saeed Kandezy,
Masoud Safarishaal, Mahshid Zoghi,
John N. Jiang
School of Electrical and Computer Engineering
the University of Oklahoma
Norman, USA

Department of Electrical and Computer Engineering
North Dakota State University
Fargo, USA
di.wu.3@ndsu.edu

Abstract—This paper presents the results of a study on the impact of coupled integrated inverter-based resources (IBRs) on the total level of harmonic distortion in a microgrid such as those powered by battery storage systems and electric vehicle charging stations. Through insensitive simulation studies with generic models of inverters and software, we analyze the relationship between the carrier frequency phase displacements in pulsewidth modulation (PWM) among coupled IBRs and the harmonic level in a microgrid. We found that the harmonic level varies in different scenarios of the phase displacements. It is also discovered that there might exist an optimal phase displacement condition under which IBRs will produce a minimum amount of harmonics. This study suggests that by appropriately coordinating the phases among coupled inverters in their PWM operation can minimize the level of harmonic distortion of total IBRs' output, while with few or no impact on the active powers of the loads in a microgrid. This could lead to low cost technical solutions to reduce the impact of harmonics on transient stability of microgrid, particularly during the fault or disturbance ridethrough periods.

Index Terms—Inverter-based resources, phase displacement, Thevenin equivalent circuit, total harmonic distortion (THD)

# I. INTRODUCTION

A high level of harmonics in a microgrid can cause various issues, such as the maloperation of protection system, expediting the aging of power equipment, and interrupting the sensitive loads, in the literature such as [1], [2]. In addition to providing active and reactive power services for microgrid reliability, inverter-based resources (IBRs) also produce a significant amount of harmonics resulting from inverter pulsewidth modulation (PWM) in a microgrid with high IBR penetration. The excessive harmonics pose great challenges to the active power related frequency stability and reactive power related voltage stability in the microgrid, particularly during transient periods as reported in [3], [4].

As suggested in many literature and reports such as [5], phases or phase displacements of inverter PWM could impact the harmonic level. Although the relationship between active and reactive power can be described by phase angle or angle displacement of synchrophasor quantities of the fundamental frequency, a quantitative description of harmonics could be very complicated, even for a simple IBR with a simple PWM algorithm. It is even more challenging to characterize the total

level of harmonics in a microgrid with a cluster or clusters of IBRs. The following is a typical example of a mathematical description of the level of harmonics of an IBR with a simple generic PWM control algorithm [6] (one of the inverters as shown in Fig. 1(a)):

$$V(t) = \sum_{n=1}^{\infty} X_n \cos(n\omega_s(t - \theta_0) - \varphi_n)$$

$$+ \sum_{m=1}^{\infty} \sum_{n=-\infty}^{\infty} W_{mn} \cos([2m\omega_c + [2n - 1]\omega_s](t - \theta_0) - \varphi_{mn})$$

$$X_n = \frac{4V_{DC}}{\pi} \frac{R}{\sqrt{R^2 + (Ln\omega_s)^2}} \frac{1}{[n\frac{\omega_s}{\omega_c}]} J_n(n\frac{\omega_s}{\omega_c} \frac{\pi}{2}M) \sin(n\frac{\pi}{2})$$

$$W_{mn} = \frac{4V_{DC}}{\pi} \frac{R}{\sqrt{R^2 + (L(2mP + [2n - 1])\omega_s)^2}} \times \frac{1}{[2m + [2n - 1]\frac{\omega_s}{\omega_c}]} J_{2n-1}([2m + [2n - 1]\frac{\omega_s}{\omega_c}]\frac{\pi}{2}M) \times \cos([m + n - 1]\pi)$$

$$\tan(\varphi_n) = \frac{Ln\omega_s}{R}$$

$$\tan(\varphi_{mn}) = \frac{L[2mP + [2n - 1]]\omega_s}{R}$$

$$P = \frac{f_c}{R}$$

where  $V_{DC}$  is the DC link voltage,  $M \in [0\ 1]$  is modulation index,  $\omega_c$  is the carrier angular frequency,  $\omega_s$  is the fundamental angular frequency,  $\theta_i$  is the phase-displacement with the given reference,  $J_n(x)$  is a Bessel function of order n and argument x, m is the carrier index, n is the beseband index, n is the load resistance, n is the line inductor and, n is the carrier to reference frequency ratio of modulation.

As shown in Equation 1, which is the mathematical description of the level of harmonics for one IBR, by aggregating a cluster of IBRs, it is very difficult to explicitly see the relationship between the phase displacements among the inverters and total harmonics level, even qualitatively, because of many interleaved variables such as R, L, different control

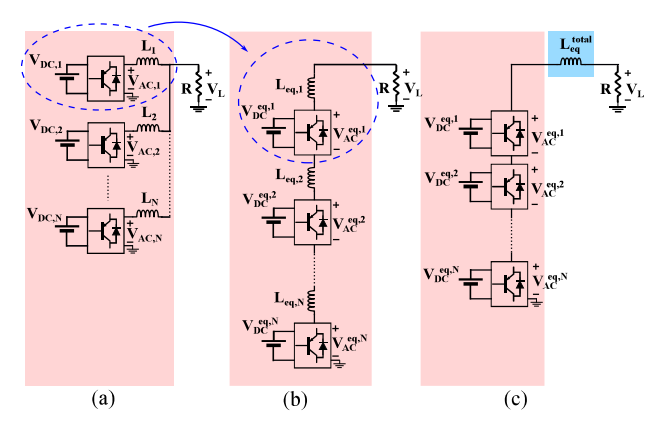


Fig. 1: Illustration of the basic IBR connection structure: (a) parallel topology, (b) equivalent cascaded topology, (c) the simple equivalent topology.

technologies, inverter topologies, etc.

The mathematical description of the output voltage of a halfbridge inverter is given in the following equation [7]:

$$V(t) = V_{DC}M\cos(\omega_0 t + \theta_0)$$

$$+ \sum_{m=1}^{\infty} \sum_{n=-\infty}^{\infty} W_{mn}\cos((m(\omega_c t + \theta_c) + n(\omega_0 t + \theta_0)))$$

$$W_{mn} = \frac{4V_{DC}}{\pi} \frac{1}{m} J_n(m\frac{\pi}{2}M)\sin((m+n)\frac{\pi}{2})$$
(2)

where  $\theta_c$  is the phase of carrier waveform,  $\theta_0$  is the phase angle of fundamental waveform. In the Equation 2, the inverter's output voltage includes fundamental component and harmonics. If the angular carrier to reference angular frequency ratio of modulation is an integer  $(\frac{\omega_c}{\omega_0} = k)$ , the carrier and baseband harmonics would be inter-harmonics with respect to the fundamental frequency. If  $\frac{\omega_c}{\omega_0}$  is not an integer, then the Equation 2 can always be written as:

$$V(t) = \underbrace{V_{DC}M\cos(\omega_0t + \theta_0)}_{\text{Fundamental component}} \\ + \underbrace{\sum_{m=1}^{\infty} \mathcal{W}_m\cos(m(k\omega_0t + \hat{\theta}_c))}_{\text{H= {High order intra-harmonic components}}} \\ + \underbrace{\sum_{m=1}^{\infty} \sum_{n=-\infty}^{\infty} \mathcal{W}_{mn}\cos((m(\omega_ct + \theta_c) + n(\omega_0t + \theta_0))}_{\text{{Harmonic components of carrier and sideband harmonics}}} \\ + \underbrace{\sum_{m=1}^{\infty} \sum_{n=-\infty}^{\infty} \mathcal{W}_{mn}\cos((m(\omega_ct + \theta_c) + n(\omega_0t + \theta_0)))}_{\text{{Harmonic components of carrier and sideband harmonics}}} \\$$

where  $\mathcal{W}_m$  and  $\mathcal{W}_{mn}$  are magnitude of intra- and interharmonics, respectively. Without losing generality,  $\hat{\theta}_c$  in Equation 3 is the characteristic phase of inverter carrier of the frequencies that belong to the synchrophasor family of the fundamental frequency where all harmonic components fully commute. Since, the high order inter-harmonics shown in Equation 3 are ignorable in most practical and analytical works, the following approximation phase relation between the fundamental and harmonics ones can be obtained.

$$V(t) \approx V_{DC} M \cos(\omega_0 t + \theta_0) + \sum_{m=1}^{\infty} W_m \cos(mk\omega_0 t + m\hat{\theta}_c)$$
(4)

As shown specifically in Equation 4, the carrier harmonics belong to the family of the fundamental component. Here,  $\theta_0$  corresponds to the phase of synchrophasor, while the  $\hat{\theta}_c$  is the characteristic phase of the inverter carrier.

Conceptually the phase of the synchrophasor  $(\theta_0)$  is used for active and reactive power control of AC energy waves at 50/60 Hz taken at a specific time marked by GPS timestamp by the phasor measurement unit (PMU) in the power grid [8]. On the contrary, the characteristic phase of individual inverter carrier  $(\hat{\theta}_c)$  is used to directly control the modulated switching operation of the inverter, expected to produce the desired level of active and reactive power at the steady state [7]. Because, the phase of inverter carrier can cause changes in the phase angle and magnitude of the output waveform, which can affect the synchronization of the measurement with the common time reference.

The relation between active and reactive power can be described by the phase angle of the synchrophasor at the fundamental frequency. The characteristic phase of the inverter carrier can define the phase angle of synchrophasor and reduce the level of harmonics in the microgrid. In the new insight, coordinating the characteristic phase of the inverters carriers make it possible to control the generated active and reactive power of inverters in the microgrid while decreasing the total level of harmonics.

For a cluster of inverters assuming  $k\hat{\theta}_c^i \approx \theta_0^i$ , conceptually, we can write,

$$V(t) = \underbrace{M \sum_{i=1}^{N} V_{DC}^{i} \cos(\omega_{0}t + \theta_{0}^{i})}_{\text{Fundamental component}} \\ + \underbrace{\sum_{i=1}^{N} \sum_{m=1}^{\infty} \mathcal{W}_{m}^{i} \cos(m(k\omega_{0}t + \hat{\theta}_{c}^{i}))}_{\text{H= {High order intra-harmonic components}}} \\ + \underbrace{\sum_{i=1}^{N} \sum_{m=1}^{\infty} \sum_{n=-\infty}^{\infty} \mathcal{W}_{mn}^{i} \cos\left(\frac{2m(\omega_{c}t + \theta_{c}^{i}) + (2n-1](\omega_{0}t + \theta_{0}^{i})}{(2n-1](\omega_{0}t + \theta_{0}^{i})}\right)}_{\text{{Harmonic components of carrier and sideband harmonics}} \notin H \text{ (inter-harmonics)}$$

where N is the number of inverters,  $V_{DC}^i$  is the  $i^{th}$  DC link voltage,  $\theta_0^i$  is the phase angle of  $i^{th}$  fundamental waveform,  $\hat{\theta}_c^i$  is the characteristic phase of  $i^{th}$  inverter carrier,  $\mathcal{W}_m^i$  is the magnitude of  $i^{th}$  intra-harmonics and  $\mathcal{W}_{mn}^i$  is the magnitude of  $i^{th}$  inter-harmonics.

In this paper, a mathematical representation for a cluster of parallelly connected IBRs is derived based on the Thevenin equivalent principle and transformation by using the known cascaded inverter structure. The derived mathematical representation provides the following useful insights: 1) the relationship between the phase displacements of inverter PWM operating at carrier frequencies among coupled IBRs and the harmonic level in a microgrid, and 2) the possible reduction of the total level of harmonics through appropriate coordination of phase displacements among IBRs. The analytical representation is verified through numerical simulations in a simple microgrid model with a generic IBR model. Moreover, the existence of grid operation condition for a minimum amount of total harmonics was discovered by the simulation experiment. This discovery suggested that it is possible to reduce the level of total harmonics by coordinating the carrier phases among inverters. Also, it suggests that the harmonic reduction via phase coordination is achievable through a cancellation effect, which will not impact the total active power outputs.

The remainder of the paper is organized as follows. Section II described the simplified representation of parallel IBRs based on the Thevenin equivalent theorem. After that, the equivalency of a cluster of IBRs with equivalent cascaded IBRs is illustrated. In section III, the results of simulation study using commonly used distribution grid and generic IBR models are presented, including the asymmetric carrier interleaving with DC link voltages in both parallel and equivalent cascaded coupling topologies. Section IV concludes the paper.

### II. ANALYTICAL DESCRIPTION OF RELATIONSHIP BETWEEN PHASE AND LEVEL OF HARMONICS

The relationship between phase displacements and the harmonics level of the total output of parallel IBRs in terms of voltage is demonstrated. Without losing generality, the discussion will be proceeded with the commonly used single-phase representation of IBRs with parallel and cascaded topologies.

# A. Explanation of the phase-harmonic relation of parallel IBRs

Fig. 1 shows the complete procedure to transfer a cluster of IBRs into a simplified equivalent cascaded IBRs based on Thevenin's circuit theorem. The general schematic of a N-parallel single-phase IBRs or the single-phase equivalent representation of the three-phase system is shown in subfigure (a). The cluster of IBRs uses various technologies, topologies, and control methods for each IBR at the power system-level. It is very complicated to account for those variations and represent a generalized mathematical model for parallel IBRs at the system-level. As shown in Equation 1, the phase and harmonic relation is not clearly shown because of structural variables such as R, L, etc. To analyze the phase and harmonics relation, we use the equivalent representation of parallel IBRs output.

The general Thevenin equivalent equation for parallel IBRs can found be as:

$$V_{AC}^{eq}(t) = \sum_{i=1}^{N} \frac{1}{N} V_{AC,i}(t) = \sum_{i=1}^{N} V_{AC}^{eq,i}(t)$$

$$L_{eq}^{total} = \frac{1}{\sum_{i=1}^{N} \frac{1}{L_i}} = \sum_{i=1}^{N} L_{eq,i}$$
(6)

where  $V_{AC}^{eq}(t)$  is the unfiltered total voltage of AC side of parallel IBRs, N is the number of parallel IBRs,  $V_{AC,i}(t)$  is the unfiltered output voltage of  $i^{th}$  IBR,  $V_{AC}^{eq,i}(t)$  is the equivalent output voltage of  $i^{th}$  equivalent cascaded IBR,  $L_{eq}^{total}$  is the total equivalent line inductances,  $L_i$  is the line inductance of  $i^{th}$  IBR and  $L_{eq,i}$  is the equivalent line inductance of  $i^{th}$  equivalent cascaded IBR.

## B. Equivalent cascaded topology of parallel IBRs

# 1) Equivalent cascaded topology obtained with Thevenin's theorem:

From the general electric circuit perspective, a cluster of coupled inverters can be considered as a set of parallelly connected voltage sources as shown in Fig. 1 (a). The equivalent circuit of N-parallel IBRs by using Thevenin's circuit theorem is shown in Fig. 1 (b). By applying Thevenin's circuit theorem, each parallel IBR in the N-parallel IBRs topology (Fig. 1 (a)) can be represented as an equivalent cascaded IBR in N-equivalent cascaded IBRs (Fig. 1 (b)). For example, DC link voltage ( $V_{DC,1}$ ) and line inductance ( $L_1$ ) of  $1^{st}$  inverter in the N-parallel IBRs topology (Fig. 1 (a)) can be represented as an equivalent DC link voltage ( $V_{DC}^{eq,1}$ ) and an equivalent line inductance ( $L_{eq,1}$ ) of  $1^{st}$  inverter in the N-equivalent cascaded IBRs topology (Fig. 1 (b)). In this regard, the structure of parallel IBRs in Fig. 1 (a) could be transformed into the equivalent cascaded IBRs, as shown in Fig. 1 (b).

#### 2) Simplified equivalent cascaded topology:

It is shown in Fig. 1 (c) that the equivalent cascaded IBRs can be simplified even more by combining all the equivalent line inductances  $(L_{eq,1}, L_{eq,2}, ..., L_{eq,N})$  to the total equivalent line inductance  $(L_{eq}^{total})$ :

$$L_{eq}^{total} = \sum_{i=1}^{N} L_{eq,i} \tag{7}$$

In Fig. 1 (c), the equivalent cascaded IBRs without total equivalent line inductance  $(L_{eq}^{total})$  has a very similar topology as a cascaded multilevel inverter. Through this transformation, the parallel IBRs are equivalent to the simplified equivalent cascaded IBRs.

In this paper, the commonly used a simple H-bridge inverter topology is used as an example to facilitate the discussion and simulations analysis and demonstrative simulation. The H-bridge inverter, as shown in Fig. 2, generates three-level output voltage including  $+V_{DC}$ , 0, and  $-V_{DC}$ . For example, the output voltage of an H-bridge inverter  $(V_H(t))$  can be explained in the form of Bessel function [7]:

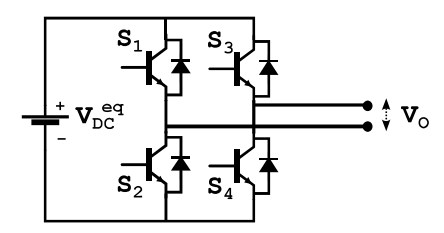


Fig. 2: The H-bridge inverter

$$V_{H}(t) = V_{DC}^{eq} M \cos(\omega_{0}t + \theta_{0}^{eq}) + \frac{4V_{DC}^{eq}}{\pi} \sum_{m=1}^{\infty} \sum_{\substack{n=-\infty\\n\neq 0}}^{\infty} \frac{1}{2m} \begin{cases} J_{2n-1}(m\pi M) \cos([m+n-1]\pi) \\ \times \cos\left(\frac{2m[\omega_{c}t + \theta_{c}^{eq}] + }{(2n-1)[\omega_{0}t + \theta_{0}^{eq}]}\right) \end{cases}$$

where  $V_{DC}^{eq}$  is the equivalent DC link voltage,  $M \in [0\ 1]$  is modulation index,  $\omega_c$  is the carrier angular frequency,  $\omega_0$  is the fundamental angular frequency,  $\theta_c^{eq}$  is the equivalent carrier phase-shift for carrier waveform,  $\theta_c^{eq}$  is the equivalent phase angle for fundamental waveform,  $J_n(x)$  is a Bessel function of order n and argument x, m is the carrier index and n is the beseband index. Due to the symmetric operating principle of most inverters at a quarter or half-cycle, the result of this simplified treatment can be applied to many other complicated inverter topologies.

By assuming the equivalent phase angle of the fundamental waveform is equal to zero for all the H-bridge inverters  $(\theta_0^{eq,1}=\theta_0^{eq,2}=...=\theta_0^{eq,N}=0)$  and all the H-bridge inverters have the same modulation index, the total output voltage of N-simplified equivalent cascaded IBRs would be:

$$V_{0}(t) = M \sum_{i=1}^{N} V_{DC}^{eq,i} \cos(\omega_{0}t) + \frac{4}{\pi} \sum_{m=1}^{\infty} \sum_{n=-\infty}^{\infty} \frac{1}{2m} \left\{ \sum_{i=1}^{N} V_{DC}^{eq,i} \cos\left(\frac{2m\omega_{c}t + [2n-1]\omega_{0}t}{+2m\theta_{c}^{eq,i}}\right) \right\}$$
(9)

With above equation, it is clearly shown the equivalent relationship between phase and harmonics level for the parallel IBRs represented based on the simplified equivalent cascaded topology. The harmonics level is impacted by equivalent carrier phase-shifts  $(\theta_c^{eq,i})$ .

In the case of equal DC link amplitudes for simplified equivalent cascaded IBRs ( $V_{DC}^{eq,1}=V_{DC}^{eq,2}=...=V_{DC}^{eq,N}=V_{DC}^{eq}$ ), the overall total harmonic distortion would be minimized if the following condition is met [5]:

$$\sum_{i=1}^{N} \cos(2m\omega_c t + [2n-1]\omega_0 t + 2m\theta_c^{eq,i}) = 0,$$

$$k = 1, 2, 3, ..., \text{ for } m \neq kN$$
(10)

Therefore, in the above condition, the minimum THD can be found by displacing each H-bridge carrier by 180/N. Under the Equation 9, the condition in the Equation 10 and equal DC link amplitudes  $(V_{DC}^{eq,1}=V_{DC}^{eq,2}=\ldots=V_{DC}^{eq,N}=V_{DC}^{eq})$ , the minimum THD can happen by displacing carrier phase-shift of the equivalent cascaded IBRs by 180/N. In this regard, the Equation 9 can be written as [9]:

$$V_{C}(t) = NV_{DC}^{eq} M \cos(\omega_{0}t) + \frac{4V_{DC}^{eq}}{\pi} \sum_{m=1}^{\infty} \sum_{n=-\infty}^{\infty} \frac{1}{2m} \begin{cases} J_{2n-1}(m\pi M) \\ \times \cos([Nm+n-1]\pi) \\ \times \cos(2Nm\omega_{c}t + [2n-1]\omega_{0}t) \end{cases}$$
(11)

In the N-simplified equivalent cascaded IBRs with equal DC links by ignoring inverters saturation at different angles, the level of harmonics are different, while the fundamental component is *almost* the same per unit-wise in terms of THD. The minimum THD can be found by displacing each H-bridge carrier by 180/N, and the DC link voltage has no effect on the minimum THD. As shown in the above equation, the phase displacement among IBRs can either increase or reduce the level of total harmonics. Note that the harmonics reduction is achieved through cancellation with appropriately coordinating phase displacements among IBRs; therefore, the active and reactive power outputs of fundamental frequency components will not change significantly.

#### III. SIMULATION RESULTS

In this section, MATLAB/Simulink simulations are conducted based on the topologies presented in Fig. 1. The level of harmonics is obtained for the topologies of simplified equivalent cascaded IBRs (subfigure(c)), and parallel IBRs (subfigure(a)) at the point of connection to the load. It is considered that both topologies have three inverters (N=3). The fundamental and carrier frequencies and load resistance are 60Hz, 1kHz, and  $1\Omega$ , respectively. To measure the total output voltage distortion, the standard THD definition is used:

$$THD = \frac{\sqrt{\left(\sum_{m=2}^{\infty} (V_m)^2\right)}}{V_1} \tag{12}$$

where  $V_1$ , m, and  $V_m$  are the magnitude of the fundamental component, harmonic order, and magnitude of harmonic, respectively. Circuit-based comparative simulation studies to verify above analysis are carried out with two types of case scenarios: 1) simulation study based on the equivalent model we derived, and 2) simulation studies based on the original parallel topology of coupled inverters.

• Case 1: simulation studies based on equivalent model (Fig. 1 (b)) and (c)). All three inverters have the same equivalent DC link amplitudes ( $V_{DC}^{eq,1} = V_{DC}^{eq,2} = V_{DC}^{eq,3} = 1p.u$ .). The equivalent carrier phase-shift of first inverter is  $\theta_c^{eq,1} = 0^{\circ}$ , while two other equivalent carrier phase-shifts ( $\theta_c^{eq,2}$  and  $\theta_c^{eq,3}$ ) are varied between

- $0^\circ < \theta_c^{eq,2} < \theta_c^{eq,3} < 180^\circ.$  The equivalent line inductances  $(L_{eq,1},L_{eq,2},L_{eq,3})$  are ignored.
- Case 2: simulation studies based on original parallel topology (Fig. 1 (a)).All three parallel IBRs have the same DC link amplitudes ( $V_{DC}^1 = V_{DC}^2 = V_{DC}^3 = 1p.u.$ ). The carrier phase-shift of first IBR is  $\theta_c^1 = 0^\circ$ , while two other carrier phase-shifts ( $\theta_c^2$  and  $\theta_c^3$ ) are varied between  $0^\circ < \theta_c^2 < \theta_c^3 < 180^\circ$ . In addition, it is assumed, the line inductances for parallel IBRs ( $L_1, L_2, L_3$ ) are negligible.

The simulation results for cases 1 and 2 for simplified equivalent cascaded IBRs and parallel IBRs with three inverters (N=3) are explained below.

## A. Experimental results and findings

# 1) Simulation study on three simplified equivalent cascaded IBRs:

The phase displacement has significant influence on the total output THD level. The contour plot in Fig. 3 demonstrates the influence. In this case, the same assumption of paralleled IBRs is considered for simplified equivalent cascaded IBRs. If the inverters' saturation is neglected, regardless of the DC links' amplitude, the minimum THD occurs as shown in Equation 10, in the  $\theta_c^{eq,1}=0^\circ$ ,  $\theta_c^{eq,2}=60^\circ$  and  $\theta_c^{eq,3}=120^\circ$ .

The curved relation in Fig. 4(a) reveals the harmonic cancellation among the simplified equivalent cascaded IBRs. Here, for the blue square color,  $\theta_c^{eq,1}=0^\circ$  and  $\theta_c^{eq,2}=60^\circ$  are kept constant and  $\theta_c^{eq,3}$  is changed from  $60^\circ-180^\circ$ . When  $\theta_c^{eq,3}=60^\circ$  or  $\theta_c^{eq,3}=180^\circ$ , maximum THD occurs but when the  $\theta_c^{eq,3}=120^\circ$ , the minimum THD happens. Same for the orange circle color,  $\theta_c^{eq,1}=0^\circ$  and  $\theta_c^{eq,3}=120^\circ$  are kept constant and  $\theta_c^{eq,2}$  is changed from  $0^\circ-120^\circ$ . When  $\theta_c^{eq,2}=0^\circ$  or  $\theta_c^{eq,2}=120^\circ$ , maximum THD occurs but when the  $\theta_c^{eq,2}=60^\circ$ , the minimum THD happens. Overall, the worst THD happens, e.g., in  $\theta_c^{eq,1}=0^\circ$ ,  $\theta_c^{eq,2}=0^\circ$  and  $\theta_c^{eq,3}=0^\circ$ . It is evident that without optimal phase displacement for simplified equivalent cascaded IBRs, THD can be high as 50%, but with optimal phase displacement, the total voltage distortion can be around 18%.

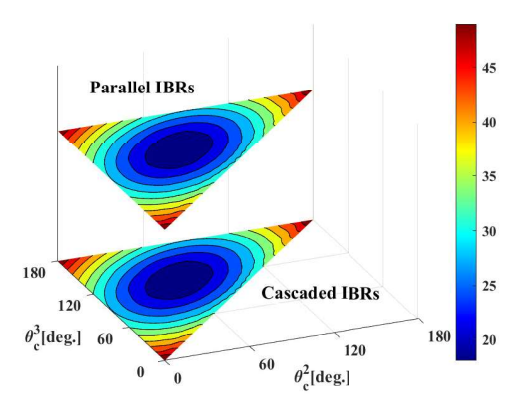


Fig. 3: Total harmonic distortion contour plot for the parallel IBRs and simplified equivalent cascaded IBRs for equal DC link voltages

2) Verification simulations with the original three parallelly coupled IBRs:

The phase displacement has a key impact on the total output THD level. The contour plot in Fig. 3 demonstrates the impact. In this simulation, carrier phase-shift of first IBR is  $\theta_c^1=0^\circ$ , while two other carrier phase-shifts ( $\theta_c^2$  and  $\theta_c^3$ ) are varied between  $0^\circ<\theta_c^2<\theta_c^3<180^\circ$ . In this case, the inverters' saturation is ignored and in addition to that, the line inductances ( $L_1,L_2,L_3$ ) are ignored. The THD contour plot for both three parallel IBRs and equivalent cascaded IBRs are very close.

The curved relation in Fig. 4(b) demonstrates the harmonic cancellation among the three parallel IBRs. The minimum THD occurs when the  $\theta_c^1=0^\circ$ ,  $\theta_c^2=60^\circ$  and  $\theta_c^3=120^\circ$ . The minimum THD is 18%. From Fig. 3 and Fig. 4(b) can be found out that with optimal phase displacement among the parallel IBRs based on Equation 10, THD would be 18% but without optimal phase displacement, THD would be as high as 50%, e.g.  $\theta_c^1=0^\circ$ ,  $\theta_c^2=0^\circ$  and  $\theta_c^3=0^\circ$ .

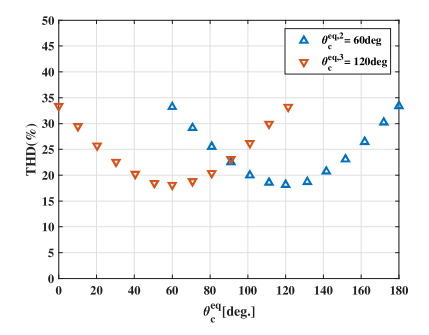
Note that as shown in of Fig. 4(c) the active power outputs of the fundamental frequency are insensitive to the carrier phase displacents. Fig. 5 presents the voltage profile for simplified equivalent cascaded IBRs and parallel IBRs with three inverters while all the DC link voltages for equivalent cascaded IBRs and parallel IBRs are equal to 1p.u., and carrier phase-shifts are equal as well ( $\theta_c^{eq,1} = \theta_c^1 = 0^\circ$ ,  $\theta_c^{eq,2} = \theta_c^2 = 60^\circ$ ,  $\theta_c^{eq,3} = \theta_c^3 = 120^\circ$ ). Both voltage profiles look alike each other, but they are not the same. Fig. 6 shows the differences between voltage profile of simplified equivalent cascaded IBRs and parallel IBRs. Both output voltages have almost the same THD (18%).

#### IV. CONCLUSION

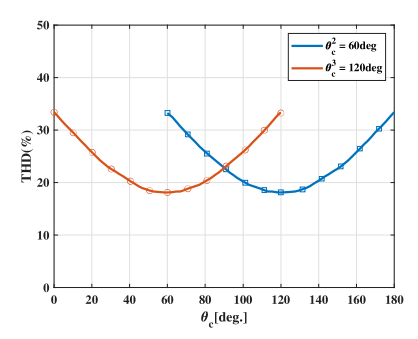
This paper studied the relationship between the phase displacements of inverter PWM operating at carrier frequencies and the harmonics level of the total output of parallel IBRs in microgrids. A model for the cluster of IBRs was derived based on the Thevenin equivalent principle with a generic model of IBR. By using this model to analyze the relationship, it is found that the phase displacement at carrier frequencies plays a very significant role in the level of harmonics. Thus, the optimal phase displacement can reduce the total voltage harmonic in the power grid under various load conditions. These results are verified and demonstrated using commonly used microgrids, inverters models, and various topological connecting structures. The optimal carrier phase displacement could be utilized to minimize the level of harmonics while the system active power of the fundamental frequency remains unchanged. The idea and concepts presented in this paper can be extended to a cluster or clusters of IBRs with different DC source voltages and a more complex coupling topology of inverters to improve total harmonic distortion in microgrids.

## ACKNOWLEDGMENT

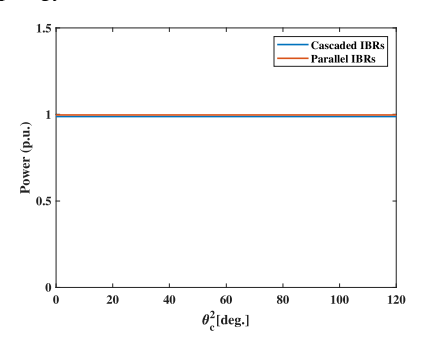
The authors express their gratitude to the funding provided to support this study from National Science Foundation (NSF),



(a) Phase displacements and harmonics relations plotted based on equivalent cascaded IBRs (Equation 1 and Equation 6).



(b) Phase displacements and harmonics relations in the actual parallel coupling topology.



(c) Phase displacements and total fundamental frequency active power outputs of coupled IBRs.

Fig. 4: Relation between phase displacements among inverters with different coupling topologies in experimental simulations (a,b); and insensitivity of fundamental frequency components to carrier phase displacement (c) for equal DC link voltages

USA EPSCoR RII Track-4 Program under the grant number OIA2033355. The findings and opinions expressed in this article are those of the authors only and do not necessarily reflect the views of the sponsors.

#### REFERENCES

- [1] Wang, Xiongfei, and Frede Blaabjerg. "Harmonic stability in power electronic-based power systems: Concept, modeling, and analysis." IEEE Transactions on Smart Grid 10, no. 3 (2018): 2858-2870.
- [2] Yang, Dongsheng, Xiongfei Wang, and Frede Blaabjerg. "Sideband harmonic instability of paralleled inverters with asynchronous carriers." IEEE Transactions on Power Electronics 33, no. 6 (2017): 4571-4577.

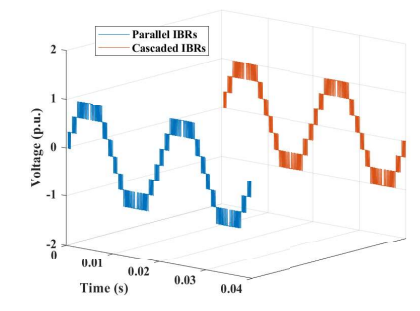


Fig. 5: Total voltage profile for parallel IBRs and simplified equivalent cascaded IBRs with three inverters for equal DC link voltages

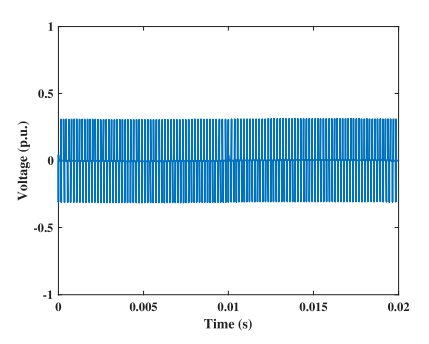


Fig. 6: Total voltage profile differences between the simplified equivalent cascaded IBRs and parallel IBRs for equal DC link voltages

- [3] Eroglu, Hasan, Erdem Cuce, Pinar Mert Cuce, Fatih Gul, and Abdulkerim Iskenderoğlu. "Harmonic problems in renewable and sustainable energy systems: A comprehensive review." Sustainable Energy Technologies and Assessments 48 (2021): 101566.
- [4] Liang, Xiaodong, and Chowdhury Andalib-Bin-Karim. "Harmonics and mitigation techniques through advanced control in grid-connected renewable energy sources: A review." IEEE Transactions on Industry Applications 54, no. 4 (2018): 3100-3111.
- [5] Monopoli, Vito Giuseppe, Youngjong Ko, Giampaolo Buticchi, and Marco Liserre. "Performance comparison of variable-angle phaseshifting carrier PWM techniques." IEEE Transactions on Industrial Electronics 65, no. 7 (2017): 5272-5281.
- [6] Benaifa, N., H. Bierk, B. Ajayi, and E. Nowicki. "Modelling and analysis of parallel operated inverters." In 2008 Canadian Conference on Electrical and Computer Engineering, pp. 001999-002002. IEEE, 2008.
- [7] Holmes, D. Grahame, and Thomas A. Lipo. Pulse width modulation for power converters: principles and practice. Vol. 18. John Wiley and Sons, 2003
- [8] Aminifar, Farrokh, Mahmud Fotuhi-Firuzabad, Amir Safdarian, Ali Davoudi, and Mohammad Shahidehpour. "Synchrophasor measurement technology in power systems: Panorama and state-of-the-art." IEEE Access 2 (2014): 1607-1628.
- [9] Holmes, Donald Grahame, and Brendan P. McGrath. "Opportunities for harmonic cancellation with carrier-based PWM for a two-level and multilevel cascaded inverters." IEEE Transactions on industry applications 37, no. 2 (2001): 574-582.